Modern Solar Facilities – Advanced Solar Science, 173–176
F. Kneer, K. G. Puschmann, A. D. Wittmann (eds.)

Velocity distribution of chromospheric downflows

R. Aznar Cuadrado*, S. K. Solanki, and A. Lagg

Max-Planck-Institut für Sonnensystemforschung, Katlenburg-Lindau, Germany
*Email: aznar@mps.mpg.de

Abstract. Infrared spectropolarimetric observations were obtained with the Tenerife Infrared Polarimeter (TIP) at the German Vacuum Tower Telescope (VTT) of the Spanish observatory of Izaña, Tenerife. We present the velocity distributions of a large dataset composed of maps of the Stokes I, Q, U, and V profiles of active and quiet sun regions obtained in the chromospheric He I 1083.0 nm triplet. The line-of-sight velocities were determined by applying a multi-Gaussian fit to the intensity profiles. Single and double component fits were carried out for all datasets. We find that 18.7% of all observed pixels show strong downflows as evidenced by a second line profile component, generally shifted by more than 8 km s^{-1} relative to the rest wavelegth. The distribution of these strong downflows displays two distinct populations. The slower one (near sonic and weakly supersonic flows) has line-of-sight velocities up to 17 km s^{-1} and is associated with moderate to strong magnetic signal (up to $\sqrt{Q^2 + U^2 + V^2}/I_c = 0.08$). Strongly supersonic downflows (reaching up to 60 km s^{-1}) are found at places with weak to moderate magnetic signal, with $\sqrt{Q^2 + U^2 + V^2}/I_c$ values mainly between 0.01 and 0.03.

1 Observations

Infrared spectroscopic observations were carried out with the Tenerife Infrared Polarimeter (TIP; Martínez Pillet et al. 1999) mounted on the German Vacuum Tower Telescope (VTT) at the Observatorio del Teide (Spain), during May 2001, October 2002, and August 2003. The spectrograph spectral resolution was 30 mÅ per pixel, and the pixel size was 0.38″. The observed wavelength range, from 1082.5 to 1083.3 nm, contains the chromospheric He I multiplet (He Ia at 1082.909 nm, He Ib at 1083.025 nm and He Ic at 1083.034 nm).

Our observations consisted of 35 scans of 13 different active regions, and 4 scans of quiet sun regions.

2 Determination of the line-of-sight velocity

We determine the line-of-sight (LOS) velocities by applying a multi-Gaussian fit to the intensity profiles. A Voigt profile, free to vary in amplitude and in a restricted wavelength interval, accounting for the telluric line at 1083.21 nm, and a linear background were also included in the fit. Single and double component fits were carried out to the chromospheric He I 1083.0 nm line for all datasets, but a second component was only considered when its amplitude exceeded 20% of that of the primary component. The existence of a second mag-

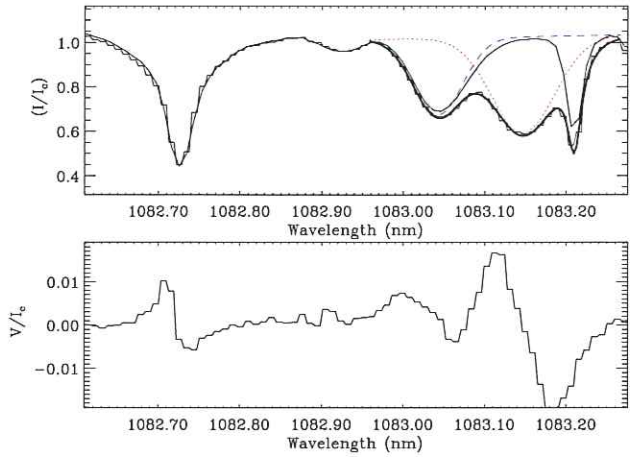

Figure 1. Stokes I and V profiles showing two different components in the chromospheric He I 1083.0 nm line of active region NOAA 10436 recorded 27 August 2003. Observed profiles are shown as histogram, dashed (blue in online version) and dotted (red) lines represent fits to the slow and fast components, respectively. The thick solid line is the fitting profile, the thin solid line in the upper frame is the average profile over the whole dataset. LOS-velocities of the two magnetic components are: $v_{slow} = -0.4$ km s^{-1} and $v_{fast} = 29.2$ km s^{-1}.

netic component was also confirmed by the presence of a magnetic signal at the position of the high velocity component in at least one of the Stokes parameters Q, U, and V.

The Doppler shifts were measured relative to the wavelength of the chromospheric He I 1083.0 nm line averaged over the whole dataset for every scanned region. The LOS velocity range is limited by the available spectral range, given basically by the size of the detector. Although occasionally strong upflows are also seen, we study here only the downflows.

In Fig. 1 we present an example of Stokes I and V profiles showing a second component in the chromospheric He I 1083.0 nm line.

3 LOS velocity distribution

In order to characterise all scanned regions, every observed dataset was divided into regions showing magnetic activity (*magnetic regions*) and no magnetic activity (*'field free' regions*). Hence, the parameter M was derived from the Stokes parameters as $M = \sqrt{Q^2 + U^2 + V^2}/I_c$ to account for the strength of the magnetic signal. The threshold for the magnetic activity classification was taken as the 3σ level of the parameter M.

In Table 1 we report the fraction of all observed pixels showing a second component, both in magnetic regions (MR, $M > 3\sigma$) and 'field free' regions (FR, $M < 3\sigma$), averaged over all observed active regions (AR) and quiet sun (QS) scans. We also show the fraction of observed pixels with downflow velocities above values from one to five times the sound speed in the chromosphere ($C_s \approx 10$ km s^{-1}, assuming a formation temperature of 10 000 K for the He I 1083.0 nm line).

Table 1. Fraction of observed pixels with a second component and fraction of observed pixels showing downflow velocities above values from one to five times the sound speed in the chromosphere, in magnetic (*MR*) and 'field free' regions (*FR*), averaged over all active regions (*AR*) and quiet sun (*QS*) scans.

		2-comp	> 10 km s^{-1}	> 20 km s^{-1}	> 30 km s^{-1}	> 40 km s^{-1}	> 50 km s^{-1}
MR	*AR*	17.97%	11.69%	2.58%	0.28%	0.03%	0.01%
	QS	0.57%	0.35%	0.06%	0.00%	0.00%	0.00%
FR	*AR*	0.13%	0.06%	0.00%	0.00%	0.00%	0.00%
	QS	0.01%	0.01%	0.01%	0.00%	0.00%	0.00%

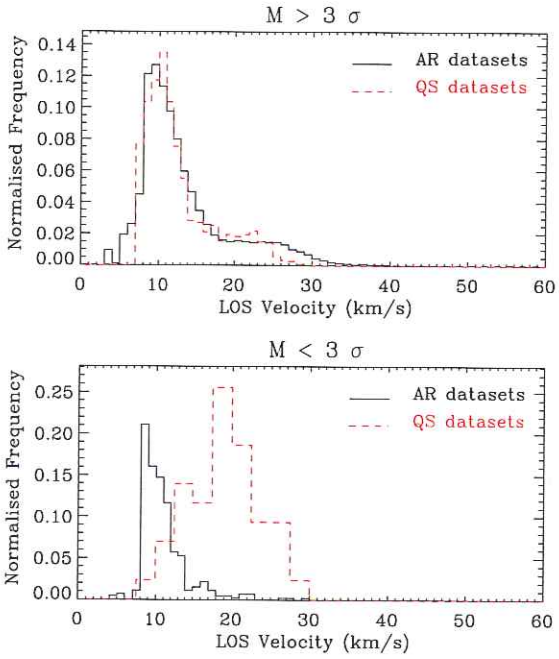

Figure 2. Histograms representing the LOS velocity distribution of downflows measured in the second component of the chromospheric He I 1083.0 nm line. Top panel: regions showing a magnetic signal ($M > 3\sigma$), bottom panel: regions not showing a magnetic signal ($M < 3\sigma$).

Fig. 2 shows the velocity distribution of downflows measured in the second component of the chromospheric He I 1083.0 nm line in *magnetic regions* (top) and *'field free' regions* (bottom), both separately analysed in active region (solid) and quiet sun (dashed) scans. The sharp lower boundary of the histograms is due to the uncertainty in fitting 2 very close components with v< 8 km s^{-1}, where a single Gaussian fit is also valid.

We find that 18.7% of all observed pixels show downflows as evidenced by a second line

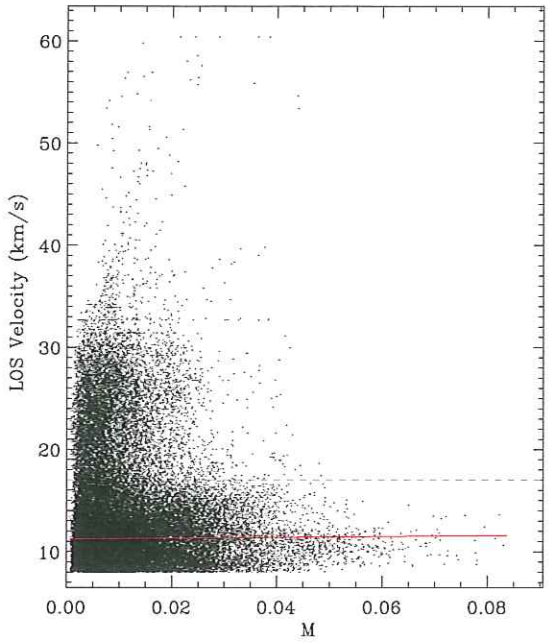

Figure 3. Scatter plot of the LOS velocities measured in the second component of the chromospheric He I 1083.0 nm line versus the magnetic field signal M. The dashed line (green in online version) represents an imaginary boundary of the two distinct populations of the chromospheric downflows distribution. The solid line (red in online version) shows a linear fit to the slower population.

profile component, while 12.1% of all observed pixels show supersonic downflows above 10 km s^{-1}. The distribution of these supersonic downflows displays two distinct populations. The slower populations peaks at around 10 km s^{-1} with line-of-sight velocities up to 17 km s^{-1}, and is associated with moderate to strong magnetic signal (up to $M = 0.08$; see Fig.3). The faster population peaks at 20 – 25 km s^{-1}. LOS velocities found in regions with no magnetic activity (i.e., $M < 3\sigma$) reach values of 30 km s^{-1}. Strongly supersonic downflows (reaching up to 60 km s^{-1}) are found at places with weak to moderate magnetic signal, with M mainly ranking between 0.01 and 0.03.

References

Martínez Pillet, V., Collados, M., Sánchez Almeida, J., et al. 1999, in High Resolution Solar Physics: Theory, Observations, and Techniques, ASP Conf. Ser., 183, 264